Brief Communication

Transient uterine hypercontractility causes oxidative stress in the fetal brain, sex-dependent mitochondrial abnormalities, and altered social behavior of adolescent male rat offspring

Arvind Palanisamy[1], Tusar Giri[1], Jia Jiang[1], Annie Bice[2], James Quirk[2], Susan E. Maloney[3], Adam Bauer[2], Joel Garbow[2], David F. Wozniak[3]

Department of Anesthesiology, Washington University School of Medicine, St. Louis, MO
Department of Radiology, Washington University School of Medicine, St. Louis, MO
Department of Psychiatry, Washington University School of Medicine, St. Louis, MO

Abstract: The neurodevelopmental impact of transient ischemic-hypoxemic insults is poorly understood. Here, we simulated placental ischemia-hypoxemia via oxytocin-induced uterine hypercontractility to show a profound decrease in placental perfusion/oxygenation, oxidative stress in the fetal brain, sex-dependent differences in gene expression mediating oxidative stress, and persistent upregulation of mitochondrial oxidative phosphorylation proteins in the anterior cingulate cortex along with social behavioral impairment especially in male offspring.

Epidemiological studies reveal a link between obstetric complications and neurodevelopmental disorders (NDD),[1-5] but the underlying biological mechanisms remain largely unexplored. Particularly, the long-term neurodevelopmental impact of transient and less severe hypoxemic insults, which are more common during labor and delivery,[6,7] is poorly understood. Here, we show that transient hypoxemia-ischemia, induced by oxytocin (OXT) induced uterine hypercontractility, causes significant oxidative stress in the fetal brain, enduring brain-region specific dysfunction of the mitochondrial electron transport chain complex, and subtle sex-dependent neurobehavioral abnormalities in the adolescent offspring.

We first quantified the effect of OXT-induced uterine hypercontractility on placental perfusion and oxygenation in term pregnant Sprague Dawley rats (E 21) with dynamic contrast-enhanced MRI and 3D multi-echo gradient echo sequence, respectively (**Fig. 1a**).[8] Placental uptake of Dotarem® contrast was approximately 40% slower post-OXT, indicating a significant decrease in uteroplacental blood flow. The average placental $R2^*$, reflecting deoxyHb concentration increased, albeit with significant location-dependent heterogeneity, suggesting that placental oxygen saturation and therefore oxygenation, was lower after OXT. Majority of these changes resolved within 20-30 min, confirming the transient nature of the insult. Consequently, we determined the impact of transient placental ischemia-hypoxemia on the developing brain by assaying for lactate and oxidative stress markers. 4 h after OXT fetal brain lactate and oxidative stress markers (4-hydroxynonenal, protein carbonyl) were significantly higher, and the antioxidant capacity (GSSG/GSH ratio) lower, confirming increased oxidative stress after transient placental hypoxemia-ischemia (**Fig. 1b**). Next, we assessed the effect of ischemia-hypoxemia on gene expression changes in the fetal cerebral cortex using RNA-seq. 24 h after OXT, only 3 genes (*mt-nd2, mt-nd4, mt-atp6*), all related to the mitochondrial electron transport chain (ETC), were found to be significantly differentially expressed (**Fig. 1c**). Notably, there was no treatment-related difference in the expression of the oxytocin receptor (oxtr) gene (Supplementary Fig 3). This

broadly suggested that the main effect of OXT-induced hypercontractility was oxidative stress and possible mitochondrial dysfunction in the fetal brain.

Considering these effects, we predicted long-term functional consequences for the fetus. Therefore, in a separate experiment, we characterized the neurobehavioral phenotype of the OXT-exposed offspring between PND 28-45 (**Fig. 2a**). Social investigation, and to a lesser extent auditory cued conditioning fear, was markedly impaired in male OXT-exposed offspring. In the observational fear learning (OFL) task, offspring of both sexes showed increased freezing behavior despite comparable baseline performance. Because there were no concomitant differences in anxiety-related behavior (elevated plus maze task), we interpreted this as heightened emotionality towards a social partner in distress. Overall, our findings suggest that transient OXT-induced uterine hypercontractility impairs sociability, especially in male offspring, and amygdalar-dependent memory. To better understand the sex differences in behavioral abnormalities, we investigated gene expression changes related to mitochondrial function and oxidative stress at an earlier timepoint — 1 h after OXT-induced uterine hypercontractility — in both male and females. Specifically, we performed planned comparisons of treatment-related differences in the expression of select target genes related to ETC/oxidative stress, anti-oxidant defense, and hypoxia/apoptosis pathways using prevalidated Taqman®-specific probes. Multiple genes were differentially expressed in a sex-dependent manner; overall, there was an increased expression of genes related to ETC/oxidative stress (*mt-nd4, mt-nd5, mt-atp8*), anti-oxidant defense (*sod2, cygb*), and hypoxia/apoptosis (*casp8, hif1a*) pathways in treated males vs. females (**Fig. 2b**). We then selectively quantified changes in proteins emblematic of these pathways with immunoblots (HIF-1alpha from nuclear extracts at 1 h, cleaved caspase-3 [CC3] from whole cortical lysates at 18 h, OXPHOS proteins in the mitochondrial fraction isolated from the anterior cingulate cortex and cerebellum at PND 28). There were no treatment or sex-related differences in either HIF-1alpha or CC3 (Supplementary fig 4), suggesting that the related gene expression changes were probably transient. However, OXPHOS proteins related to mitochondrial ETC complex I, III, and IV were selectively higher in the anterior cingulate cortex, but not the cerebellum, of PND 28 male OXT-exposed offspring (**Fig. 2c**). Given the importance of the anterior cingulate cortex in both social and empathy-related behavior,[9-11] we speculate that the sex differences in behavior may be partly related to altered expression of proteins related to mitochondrial ETC in this region. To determine if there were consequences for functional connectivity (FC), we performed FC analysis with optical intrinsic signaling (OIS) in a separate cohort of male offspring.[12] Among the brain regions that could be meaningfully studied, we detected significant differences in FC only in the somatosensory cortex of OXT-exposed male pups (**Fig. 2d**).

In conclusion, transient intrauterine ischemia-hypoxemia was associated with male-specific differences in social behavior, expression of selective oxidative stress genes in the developing cortex, and enduring upregulation of mitochondrial ETC proteins in the anterior cingulate cortex. Collectively, our findings support the possibility of persistent mitochondrial dysfunction as a mechanistic link between transient intrauterine asphyxia and NDD and identify the anterior cingulate cortex as a brain region of susceptibility and significance.

Methods

1. Animals and Drugs: All experiments reported here were approved by the Institutional Animal Care and Use Committee at Washington University in St. Louis (#20170010) and comply with the ARRIVE guidelines. Timed pregnant Sprague Dawley (SD) rats (Charles River Laboratories, Wilmington, MA) were used for all experiments. Oxytocin (OXT; Selleck Chemicals, Houston, TX) was prepared as a 1mg/mL solution in sterile normal saline. We developed a rapid method to identify the sex of the pups using visual inspection of the anogenital distance at E21. Another experimenter cross-checked and verified the sex by performing a mini-laparotomy to identify the presence (male) or absence (female) of testes and seminal vesicles (Supplementary figure 1).

2. Placental imaging: SD dams at E21 were anesthetized with isoflurane in 100% oxygen and imaged on an Agilent (Santa Clara, CA) 4.7T DirectDrive MRI system using a 7.2 cm inner diameter quadrature RF coil. For all rats, anatomic scans were initially acquired across the entire abdomen using a respiratory-gated 2D fast spin echo sequence (FSEMS). Placental R2* mapping was performed on 4 SD dams using a 3D multi-echo gradient echo sequence to measure changes in deoxyhemoglobin concentration. In 3 dams, placental blood flow was measured by dynamic contrast enhanced (DCE) MRI during and after a tail vein injection of Dotarem® (Guerbet, Princeton, NJ, 0.2 mmol/kg). The rats were then injected with either 100 μg/kg of OXT to induce uterine contraction or an equivalent volume of saline through a 22G tail vein catheter. Following the cessation of gross abdominal motion, typically around 30 min as assessed by non-gated low-resolution scouts, the anatomic scan was re-acquired to account for placental displacement during the contraction period and the R2* or DCE measurement was repeated. For the saline-injected rats, a 30 min delay was observed prior to acquiring post-injection scans. Placental perfusion was quantified with using the initial area under the curve (AUC) approach and washout slope of the DCE time-intensity curve. Rat placentas were manually segmented from pre- and post-OXT images using customized MATLAB routines, and optimal estimates of R1 and R2* were determined for each placenta using software implementing Bayesian probability theory. For anatomic scans: 2D multi-slice Fast Spin Echo (0.5 x 1 x 1 mm^3 resolution, zero-padded to 0.5 x 0.5 x 1 mm^3, TR/TE = 2000/48 ms, echo train length = 4, 4 averages, respiratory gated, imaging time approximately 6 min depending upon respiration rate). For R2* mapping: 3D multi-echo gradient echo (0.75 mm isotropic resolution, TR/TE/ΔTE = 40/1.7/4 ms, 6 echoes, flip angle = 15 degrees, 4 min 16 sec). DCE: 2D multi-slice gradient echo (1 x 1 x 2 mm^3resolution, 12 slices, TR/TE = 46.8/1.79 ms, flip angle = 90 degrees, 3 second temporal resolution, repeated for 10 min, injection at 1 min).

3. Lactate assay: To determine if OXT-induced uterine contractions induce hypoxemia in the fetal brain, we assayed for fetal brain lactate 4 h after 100 μg/kg i.v OXT or saline in timed pregnant E21 Sprague Dawley (SD) dams (n = 8 each). Briefly, whole male and female fetal brains were homogenized on ice and deproteinized with 10 kDa molecular weight cut-off spin filter to remove lactate dehydrogenase. Protein concentrations were determined using BCA Protein Assay Kit (ThermoFisher Scientific), followed by lactate assay (Lactate Colorimetric Assay Kit II; Sigma-Aldrich) according to manufacturer's instructions. Results calculated from standard curve are expressed as nmoL/mg brain protein. Outliers were detected and eliminated using ROUT (robust regression and outlier analysis) with Q set to 10%. Normality of residuals was checked with

D'Agostino-Pearson omnibus test followed by 2-way ANOVA and Sidak's multiple comparisons test to assess for significant sex-dependent differences in the treated group. Data presented as mean ± SEM.

4. Oxidative stress assays: To determine if OXT causes oxidative stress in the fetal brain, we assayed male and female fetal brains for 4-hydroxynonenal (4-HNE, a byproduct of lipid peroxidation), protein carbonyl, and the antioxidant GSSG/GSH in the same E21 dams used for the lactate assay. Briefly, whole fetal brains were homogenized in PBS buffer on ice. Protein concentrations were determined using BCA Protein Assay Kit (Thermo Scientific), followed by 4-HNE assay (OxiSelect™ HNE Adduct Competitive ELISA Kit;), protein carbonyl (OxiSelect™ Protein Carbonyl ELISA kit), and total glutathione assay (OxiSelect™ GSSG/GSH Assay Kit) according to manufacturer's instructions. All assays were supplied by Cell Biolabs, Inc, San Diego, CA. Results calculated from the standard curve are expressed as mcg/mg of brain protein. Outliers were detected and eliminated using ROUT (robust regression and outlier analysis) with Q set to 10%. Normality of residuals was checked with D'Agostino-Pearson omnibus test followed by 2-way ANOVA and Sidak's multiple comparisons test to assess for significant sex-dependent differences in the treated group. Data presented as mean ± SEM.

5. RNA-sequencing: E21 timed pregnant SD rats were treated with either 100 µg/kg OXT or saline through a 22G tail vein catheter (n = 5 each). 24 h later, fetal brains were harvested under isoflurane anesthesia. Total RNA was extracted the right cerebral cortex using RNAeasy kit (Qiagen). Only RNA with RIN > 9.5 were used for RNA-seq. RNA-seq reads were aligned to the Ensembl top-level assembly with STAR version 2.0.4b. Gene counts were derived from the number of uniquely aligned unambiguous reads by Subread: featureCount version 1.4.5. Transcript counts were produced by Sailfish version 0.6.3. Sequencing performance was assessed for total number of aligned reads, total number of uniquely aligned reads, genes and transcripts detected, ribosomal fraction known junction saturation and read distribution over known gene models with RSeQC version 2.3.All gene-level and transcript counts were then imported into the R/Bioconductor package EdgeR and TMM normalization size factors were calculated to adjust for samples for differences in library size. Genes or transcripts not expressed in any sample were excluded from further analysis. The TMM size factors and the matrix of counts were then imported into R/Bioconductor package Limma and weighted likelihoods based on the observed mean-variance relationship of every gene/transcript and sample were then calculated for all samples with the voomWithQualityWeights function. Performance of the samples was assessed with a spearman correlation matrix and multi-dimensional scaling plots. Gene/transcript performance was assessed with plots of residual standard deviation of every gene to their average log-count with a robustly fitted trend line of the residuals. Generalized linear models were then created to test for gene/transcript level differential expression. Differentially expressed genes and transcripts were then filtered for FDR adjusted p-values ≤ 0.2.

6. Behavioral experiments: Male and female offspring of E21 SD dams (n = 9 each) treated with OXT (100 µg/kg) or saline (OXY or SAL rats, respectively) were subjected to behavioral testing. There were no differences in litter size, sex ratio, and survival of the offspring from both treatment groups. Pups were weaned on P21 and subsequently evaluated on a battery of behavioral tests from postnatal day (PND) 26-45 in the following order: 1) 1h open field; 2) social approach; 3) elevated plus maze; 4) observational fear learning;[13] and 5) conditioned fear. The OXT and SAL rats were

tested in two cohorts (n = 6 and 3 dams each, respectively) for which identical behavioral protocols were used. However, conditioned fear was only conducted on the second cohort of rats. A total of 12 male and female offspring from the OXT and SAL group were tested. Details of all behavioral experimental procedures are included in the supplementary file and described previously.[14] Data were analyzed with 2-way ANOVA, followed by a simple main effects test if the interaction term was significant. Data presented as mean ± SEM.

7. Taqman qPCR: Male and female fetal brains exposed to either 100 μg/kg OXT (n = 8) or saline (n = 8) *in utero* were harvested and immediately stored at -80 °C. RNA was extracted using RNeasy plus mini kit (Qiagen), converted to cDNA using SuperScript® IV VILO™ master mix kit (Invitrogen), and 25 ng of the template cDNA was then combined with a ready-to-use TaqMan Fast Advanced qPCR Master Mix (Thermo Fisher Scientific, Waltham, MA) for experiments in a pathway-specific custom TaqMan array (Custom TaqMan® Array Fast Plate 96, Life Technologies, Carlsbad, CA). Expression levels of 28 genes relevant to three specific pathways mitochondrial electron transport chain (ETC) complexes (*mt-cyb, mt-nd1, mt-nd2, mt-nd4, mt-nd5, mt-atp6, mt-atp8, mt-co1, mt-co3, nox4, nos2)*, oxidative stress and anti-oxidant defense (*cat, gpx1, gpx2, gsr, prdx1, sod1, sod2, srxn1, nqo1, mt3, cygb*), and hypoxia, stress and toxicity (*bax, bcl2l1, casp8, hif1a, nfkb1*) were assayed in triplicate along with four endogenous housekeeping control genes (*18S rRNA, gapdh, pgk1,* and *actb*). Thermal cycling was performed in 7500 Fast Real-Time PCR System (Applied Biosystems®, Foster City, CA) and the threshold cycle (Ct) values for all genes were calculated using proprietary software. We tested the experimental stability of all 4 endogenous reference genes using the geNorm algorithm and determined *pgk1* to be the most stable reference gene. Relative mRNA expression, normalized to *pgk1*, was calculated using the $2^{-\Delta\Delta CT}$ method with sex-matched control samples as reference. Outliers were detected and eliminated using ROUT (robust regression and outlier analysis) with Q set to 10%. Normality of residuals was checked with D'Agostino-Pearson omnibus test followed by 2-way ANOVA and Sidak's multiple comparisons test to assess for significant sex-dependent differences in the treated group. Data with non-normal residuals (*mt-atp6, mt-co1, nox4, cat, gsr, prdx1, sod2, bcl2l1, hif1a*) were Box-Cox transformed prior to statistical testing. Data presented as mean ± SEM.

8. Western blotting: Fetal cortical lysates (≈100 mg) were extracted using RIPA buffer (50 mM Tris HCl pH 7.5, 150 mM NaCl, 2 mM EDTA, 1% NP40, 0.1% SDS) with protease and phosphatase inhibitor cocktail (ThermoFisher Scientific Inc). Mitochondrial and nuclear fractions from the fetal cortex were separately prepared using appropriate kits (mitochondrial isolation kit, catalog # 89801 and subcellular protein fractionation kit, catalog # 87790, ThermoFisher Scientific Inc) following manufacturer's instructions. Approximately 30 μg of protein was subjected to gel electrophoresis and transferred to membrane using Bolt western blot reagents from ThermoFisher Scientific Inc (bolt 4-12% Bis Tris gel, catalog # NW04125; bolt sample reducing agent, catalog # B0009; bolt LDS sample buffer, catalog # B0007; iBlot2 dry blotting system). Membranes were blocked with TBST buffer (catalog # S1012, EZ Bioresearch), containing 5% milk for 1 hour at room temperature on a shaker. Following a brief wash with TBST buffer, the membranes were immunoblotted overnight at 4 °C on a shaker with antibodies against hif1a (Catalog # 14179, Cell Signaling Technology), cleaved caspase 3 (Asp-175) (Catalog # 9661, Cell Signaling Technology), OXPHOS rodent ab cocktail (ab110413) (Catalog # MS604300, Abcam Inc). Beta-actin (Catalog # MA5-11869, ThermoFisher Scientific Inc), VDAC1 (Catalog # ab 15895, Abcam Inc), and histone H3 (Catalog # 9715S, Cell Signaling Technology) were used for normalization.

For OXPHOS experiments, rat heart mitochondria were used as positive control. All the primary antibodies were used at a dilution of 1:1000. HRP-conjugated secondary antibodies (anti-Rab IgG, catalog #7074 and anti-mouse IgG, catalog #7076, Cell Signaling Technology) were used at a dilution of 1:1000 for 1 hour at room temperature on a shaker. Immunoblots were incubated with Western ECL substrate (catalog # 1705060, Bio-Rad Inc) for 5 minutes at room temperature, followed by exposure to film inside a cassette in dark room, and developed using Konica Minolta Inc, Film Processor (catalog # SRX-101A). Western blot images were processed with ImageJ for densitometric quantification.

9. Functional connectivity analysis: Functional connectivity of the brain of OXT-exposed male offspring was assessed at P23 using a reflectance-mode functional connectivity optical intrinsic signal (fcOIS) imaging system.[12] The fcOIS system images the brain through the intact skull and records spontaneous fluctuations in oxy- and deoxyhemoglobin. Through neurovascular coupling, these fluctuations represent spatio-temporal variations in neural activity, similar to human BOLD-fMRI. Quantitative differences in homotopic fc in 7 brain regions were compared as shown in Fig 2d. Significant differences in fc was observed only for the somatosensory cortex. Data were analyzed with student's t-test and presented as mean ± SEM.

Figure and Figure Legends

Figure 1

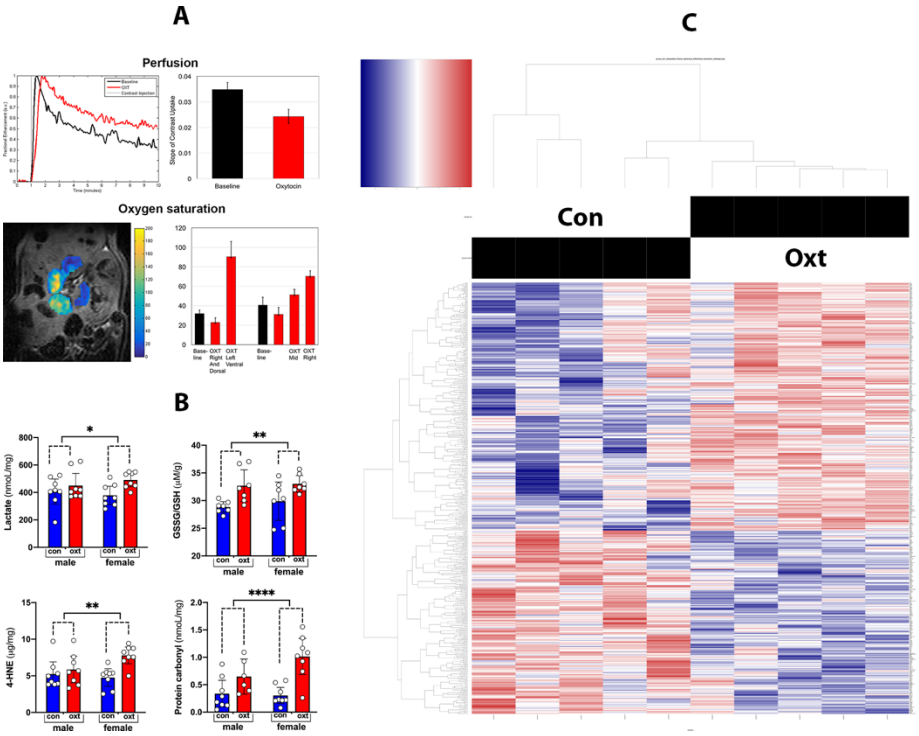

Figure 1: a.) Placental perfusion and oxygenation are impaired after OXT-induced uterine hypercontractility: Top panel: perfusion. Left - normalized contrast uptake curve from one slice of a placenta at baseline (black) and post-OXT (red), illustrating the reduced placental perfusion post-OXT; right - slope of the normalized signal enhancement curve following Dotarem® injection averaged across all placentas at baseline (black) and post-OXT (red). Bottom panel: placental oxygenation**:** Left – a representative post-OXT placental R2* map overlaid on a FSEMS image in an E21 dam, illustrating differences in placental R2* across the abdomen. Right – Average placental R2* values for each rat at baseline and after OXT. The post-OXT placentas are divided into 2-3 groups based upon their spatial location within the abdomen. All comparisons within a rat are statistically significant (*$p < 0.05$), except for rat 2 baseline vs. OXT left. **b.) Increased oxidative stress in the fetal brain after OXT-induced uterine hypercontractility:** *In utero* exposure to OXT-induced uterine hypercontractility was associated with an increase in fetal brain lactate (*$p = 0.02$), 4-hydroxynonenal (**$p = 0.007$), protein carbonyl (****$p < 0.0001$), and oxidized GSSG/GSH (**$p = 0.001$) at 4 h suggestive for oxidative stress. Data analyzed with 2-way ANOVA and presented as mean ± SEM**.** *$p < 0.05$, **$p < 0.01$, ***$p < 0.001$, ****$p < 0.0001$. **c.) Changes in the fetal cortical transcriptome after OXT-induced uterine hypercontractility:** Heat map showing differential expression of cortical genes in E21 offspring from OXT-treated and control dams (n=5 each). Of the 584 genes that were differentially expressed, only 3 genes (*mt-nd2, mt-nd4, mt-atp6*) passed the FDR adjusted p-value cutoff of ≤ 0.2.

Figure 2

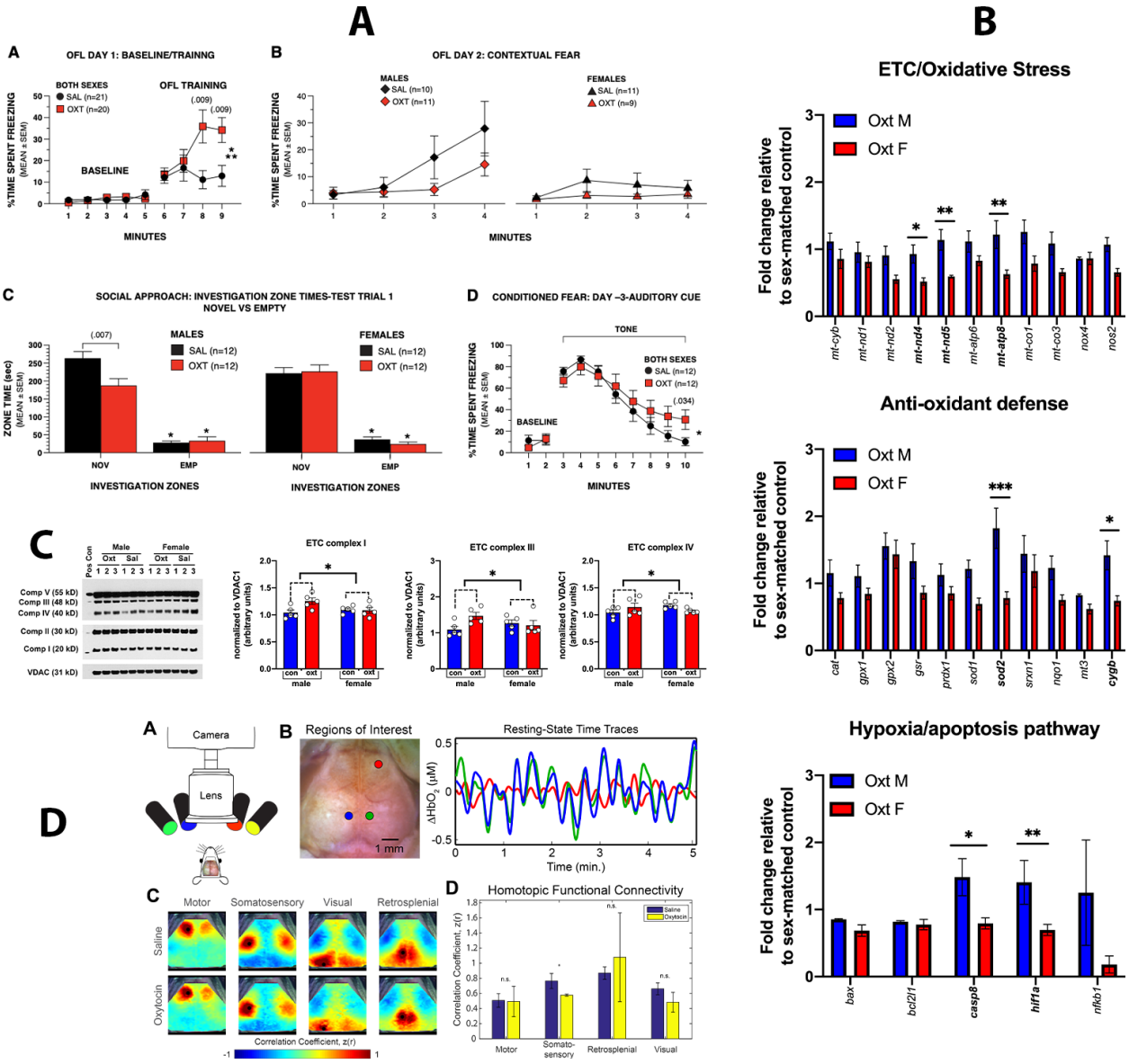

Figure 2: a.) OXT-induced uterine hypercontractility causes heightened emotionality and male-specific impairment of social behavior. A. OXT offspring showed greatly increased freezing levels in the OFL during the last 2 min of training suggesting an enhanced empathy-like response (treatment effect, *p = 0.04; treatment x min interaction, **p = 0.003).B. OFL contextual fear yielded a sex effect (*p = 0.04) without an effect of treatment. C. Male SAL rats spent significantly more time investigating the novel rat compared to the OXT rats (**p=0.007). No differences between females were observed. D. A significant treatment x min interaction was found for auditory cue fear conditioning (*p=.02). **b.) Sex-dependent gene expression changes in the fetal cerebral cortex 1 h after OXT-induced hypercontractility.** Multiple genes were differentially expressed in a sex-dependent manner after OXT-induced hypercontractility. Overall,

there was an increased expression of genes related to ETC/oxidative stress (*mt-nd4, mt-nd5, mt-atp8*), anti-oxidant defense (*sod2, cygb*), and hypoxia/apoptosis (*casp8, hif1a*) pathways in treated males vs. females. *p < 0.05, **p < 0.01, and ***p < 0. 001. **c.) Enduring upregulation of OXPHOS proteins in the anterior cingulate cortex of male offspring after *in utero* OXT.** Representative immunoblots of anterior cingulate cortex homogenates from P28 offspring showing increased expression of proteins related to the mitochondrial electron transport chain (OXPHOS). Scatter plots show a significant increase in complexes I (*p=0.04 for treatment x sex interaction; F (1, 16) = 5.3), III (*p=0.05 for treatment x sex interaction, F (1, 16) = 4.6), and IV (*p=0.04 for treatment x sex interaction, F (1, 16) = 5.1) in the male offspring. Normalization was done with mitochondrial VDAC1 protein. **d.) Functional connectivity analysis:** A) Four LEDs (470 nm, 530 nm, 590 nm, and 625 nm) illuminate the dorsal surface of the intact rat skull. A 75mm f/2.8 lens and back-illuminated EMCCD sensor collect diffuse light reflected from the brain. B) Example regions of interest reveal spontaneous hemodynamic activity over a 5-minute imaging session. Notice the temporal coherence between the blue and green regions compared to the red region. Correlating spontaneous fluctuations in each region with all other brain pixels creates a functional connectivity map. C) FC maps in 4 brain regions (black dots) in P23 male rat offspring exposed to OXT-induced hypercontractility (n = 4) or saline (n = 3) *in utero*. Red pixels denote high positive functional connectivity with seeded region. D) Quantitative comparisons of regional homotopic FC reveal significant group differences in the somatosensory cortex; *p < 0.05.

References

1. Kolevzon A, Gross R, Reichenberg A. Prenatal and perinatal risk factors for autism: a review and integration of findings. *Arch Pediatr Adolesc Med.* 2007;161(4):326-333.
2. Glasson EJ, Bower C, Petterson B, de Klerk N, Chaney G, Hallmayer JF. Perinatal factors and the development of autism: a population study. *Archives of general psychiatry.* 2004;61(6):618-627.
3. Dalman C, Thomas HV, David AS, Gentz J, Lewis G, Allebeck P. Signs of asphyxia at birth and risk of schizophrenia. Population-based case-control study. *Br J Psychiatry.* 2001;179:403-408.
4. Cannon M, Jones PB, Murray RM. Obstetric complications and schizophrenia: historical and meta-analytic review. *Am J Psychiatry.* 2002;159(7):1080-1092.
5. Modabbernia A, Mollon J, Boffetta P, Reichenberg A. Impaired Gas Exchange at Birth and Risk of Intellectual Disability and Autism: A Meta-analysis. *J Autism Dev Disord.* 2016;46(5):1847-1859.
6. Heuser CC, Knight S, Esplin MS, et al. Tachysystole in term labor: incidence, risk factors, outcomes, and effect on fetal heart tracings. *American journal of obstetrics and gynecology.* 2013;209(1):32 e31-36.
7. Kunz MK, Loftus RJ, Nichols AA. Incidence of uterine tachysystole in women induced with oxytocin. *J Obstet Gynecol Neonatal Nurs.* 2013;42(1):12-18.
8. Tomlinson TM, Garbow JR, Anderson JR, Engelbach JA, Nelson DM, Sadovsky Y. Magnetic resonance imaging of hypoxic injury to the murine placenta. *Am J Physiol Regul Integr Comp Physiol.* 2010;298(2):R312-319.
9. Apps MA, Rushworth MF, Chang SW. The Anterior Cingulate Gyrus and Social Cognition: Tracking the Motivation of Others. *Neuron.* 2016;90(4):692-707.
10. Hadland KA, Rushworth MF, Gaffan D, Passingham RE. The effect of cingulate lesions on social behaviour and emotion. *Neuropsychologia.* 2003;41(8):919-931.
11. Carrillo M, Han Y, Migliorati F, Liu M, Gazzola V, Keysers C. Emotional Mirror Neurons in the Rat's Anterior Cingulate Cortex. *Curr Biol.* 2019;29(8):1301-1312 e1306.
12. Bauer AQ, Kraft AW, Wright PW, Snyder AZ, Lee JM, Culver JP. Optical imaging of disrupted functional connectivity following ischemic stroke in mice. *Neuroimage.* 2014;99:388-401.
13. Kim A, Keum S, Shin HS. Observational fear behavior in rodents as a model for empathy. *Genes Brain Behav.* 2019;18(1):e12521.
14. Maloney SE, Yuede CM, Creeley CE, et al. Repeated neonatal isoflurane exposures in the mouse induce apoptotic degenerative changes in the brain and relatively mild long-term behavioral deficits. *Sci Rep.* 2019;9(1):2779.

Supplemental file

1. Rapid sex determination of E21 offspring

We developed a confirmatory test to establish the sex of E21 pups by performing a mini-laparotomy to identify the presence (males) or absence (females) of testes. Testes can be identified as a globular structure covered with tortuous vasculature (marked with white circle). Performed in conjunction with visual inspection of the anogenital distance, we were able to achieve 100% accuracy with sex identification.

Supplementary Figure 1

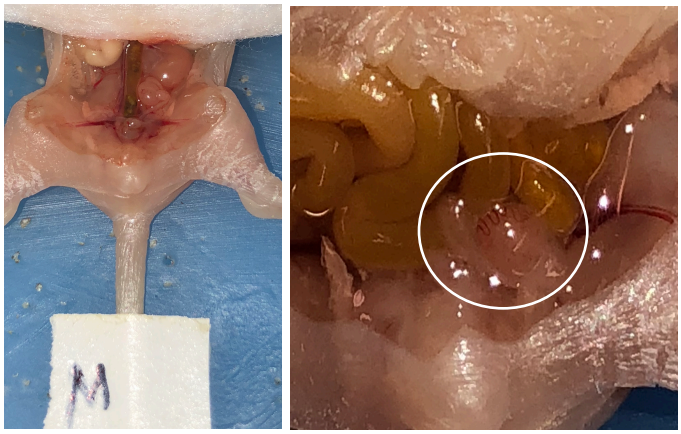

2. Behavioral experiments

1 h open-field activity: On PND 31 the OXT and SAL rats were evaluated in terms of general ambulatory activity and exploratory behavior over a 1 h period in an open-field (41 x 41 x 38.5 cm high) constructed of Plexiglas and containing computerized photobeam instrumentation (Kinder Scientific, LLC, Poway, CA). The apparatus included a frame that housed a 16 x 16 matrix of photocell pairs at ground level to quantify horizontal movement as well as another frame that contained 16 photocell pairs on its long axis, which was raised approximately 8.5 cm above the floor to measure vertical rearing behavior. General activity variables included total ambulations (whole body movements), vertical rearing frequency, and distance traveled in a 5.1 cm wide peripheral zone that surrounded the field. Classic measures of emotionality involved quantifying time spent in, distance travelled in, and number of entries made into a 10.2 x 10.2 cm central zone of the field.

Social approach: The day after being tested in the open field, the performance of the juvenile rats was assessed on the social approach measure, which was used to quantify sociability (tendency to initiate social contact with a novel conspecific), and preference for social novelty (tendency to initiate social contact with a novel versus a familiar conspecific). For the present studies we used our previously published protocol for mice, although the apparatus used was of a size scaled for rats. Specifically, the apparatus was a rectangular 3-chambered Plexiglas box (Stoelting Co., Wood Dale, IL.) with each chamber measuring 33 cm (w) x 100 cm (l) x 22 cm (h) containing Plexiglas dividing walls with square openings (10 x 10 cm). A withholding cylinder [30 cm (h); 16.5 cm

diam] that contained vertical bars was used to sequester a stimulus rat. The presence of vertical bars allowed for minimal contact between rats but prevented fighting or sexual behaviors, and one was located in each outer chamber. A digital video camera connected to a PC computer that contained a tracking software program (ANY-maze, Stoelting Co., Wood Dale, IL.) that recorded the movement of a rat within the apparatus and quantified time spent, latency to enter, number of entries and distance traveled in each chamber, as well as time spent, latency to enter and number of entries made into an investigation zone surrounding each cylinder. The investigation zones were 20.5 cm in diameter, encompassing 2 cm around the withholding cylinders. An entry into the chambers was defined when a chamber contained 80% of the rat's body, while only the head was tracked in the zones surrounding the withholding cylinders to capture investigative social behaviors. Indirect lighting illuminated the test room and the entire apparatus was cleaned with Nolvasan solution while the cylinders were cleaned with 75% ethanol solution between tests.

Each test session consisted of 3 consecutive 10-min trials, the first trial being dedicated to habituation to the apparatus and general procedure, with the second two being test trials. For the first trial, each rat was placed in the middle chamber for acclimation to the entire apparatus. During the first trial, a rat was allowed to freely investigate and habituate to all three chambers, including the empty withholding cylinders. The second trial (test trial 1) involved placing an unfamiliar, sex-matched conspecific in one withholding cylinder, while the other was left empty, and the test rat was allowed to freely explore the apparatus and investigate the novel stimulus rat in the cylinder. For the third trial (test trial 2), the stimulus rat was left in the withholding cylinder same location while a novel rat was placed in the other cylinder and the test rat was allowed to explore the apparatus and investigate the two rats contained in the cylinders. Locations of the stimuli rats in the outer chambers for the test sequences were counterbalanced within and across groups. Entries, latency to enter, and time spent in each of the investigation zones and chambers were recorded for each rat.

Elevated plus maze (EPM): Three days after completing social approach testing, anxiety-like behaviors were evaluated in the EPM according to our previously described procedures for rodents. Given the young age and size of the juvenile rats in the study and the fact that we were using a 3-day protocol, the decision was made to use our mouse version of the apparatus instead of our apparatus that is used with adult rats. The entire apparatus was thoroughly cleaned with 70% EtOH prior to testing. Conditioned aversion to the open arms becomes strong across the 3 days of testing and we wanted to encourage at least a modest level of exploration of the open arms during the second and third test sessions to avoid "floor effects". The apparatus consisted of two opposing open arms and two opposing enclosed arms (36 x 6.1 x 15 cm) that extended from a central platform, (5.5 x 5.5 cm) which were constructed of black Plexiglas. The maze was equipped with pairs of photocells configured in a 16 (x-axis) x 16 (y-axis) matrix, the output of which was recorded by a computer and interface assembly (Kinder Scientific, Poway, CA, USA). A system software program (MotorMonitor, Kinder Scientific, Poway, CA, USA) enabled the beam-break data to be recorded and analyzed to quantify time spent, distance traveled, and entries made into the open and closed arms and center area. To adjust for differences in general activity, the percentage of distance traveled, time spent, and entries made in the open arms out of the totals (open arms + closed arms) for each variable were also computed. Test sessions were conducted in a dimly lit room with light being provided by two 13-watt black-light bulbs (Feit EcoBulbs). Each

5-min session began by placing a rat in the center of the maze and allowing it to freely explore the apparatus, with testing being conducted over 3 consecutive days.

Observational fear learning (OFL): On the two consecutive days following completion of EPM testing, empathy-like fear responses were assessed in the OFL task by conditioning the rats to context-dependent fear as a result of observing a conspecific receiving repetitive foot shocks, based on previously published procedures. The apparatus (27cm x 31cm x 30.5cm) consisted of an acrylic chamber with a stainless-steel grid floor equipped with a house light, video camera, and contained within a sound-attenuating chamber (Lafayette Instrument Co. and Actimetrics). One half of the apparatus contained a custom clear acrylic stimulus chamber (13cm x 24.5cm x 20cm) with 90, 1cm diameter holes on one side to allow for scent and sound penetration and no floor to allow for exposure to shock. A matte PVC cover was placed over the grid floor in the other half of the chamber, designated the observer compartment, to prevent the test rat from receiving foot shocks. On day 1, a stimulus rat was placed in the stimulus chamber and an observer test rat was placed in the observer compartment. Baseline freezing behavior of the observer test rat was quantified for 5 minutes. During minutes 6-9, the stimulus rat received a 2s 1.0mA footshock every 10s, and the freezing behavior of the observer test rat was quantified. On day 2, the observer test rat was again placed in the observer compartment and freezing behavior was quantified over the 4 min test to evaluate the contextual fear response in the absence of the stimulus rat. Freezing (no movement except for that associated with respiration) was quantified using FreezeFrame (Actimetrics, Evanston, IL), which allowed for the simultaneous visualization of behavior while adjusting a "freezing threshold" which categorized behavior as "freezing" or "not freezing" during 0.75 s intervals. The dependent variable analyzed from both trials was the percent of time spent freezing.

Conditioned fear: In the second cohort of OXT and SAL rats – but not the first cohort -- the conditioned fear procedure was conducted three days after completing OFL testing using a procedure similar to previously published methods (Thio et al., 2010). The rats were trained and tested in four Plexiglas conditioning chambers (27cm x 31cm x 30.5cm high) (Lafayette Instrument Co. and Actimetrics) containing different visual, odor, and tactile cues. On day 1, each rat was placed into the training/test chamber and freezing behavior was quantified during a 2 min baseline. After this a conditioned stimulus (CS) in the form of an 80-dB tone (white noise) was presented for 20 s. During the last second of the CS, a 1.0 mA foot shock (unconditioned stimulus; US) was administered. This pairing was repeated for each of the next 2 min for a total of 3 CS-US pairings. The following day the rats were placed back into the same training/test chamber, which contained the same set of cues, and freezing behavior quantified over 8-min to evaluate contextual fear conditioning in the absence of the tone or shock. On the third day (24 h later), the rats were placed into a second chamber containing different cues and freezing behavior was quantified for a 2-min “altered context” baseline and over the subsequent 8 min, during which time only the tone was presented. Freezing (no movement except for that associated with respiration) was quantified using FreezeFrame (Actimetrics, Evanston, IL), in the same manner as described above for the OFL procedure. The dependent variable analyzed from all trials was the percent of time spent freezing. Shock sensitivity was evaluated following completion of the conditioned fear testing.

Supplementary Figure 2

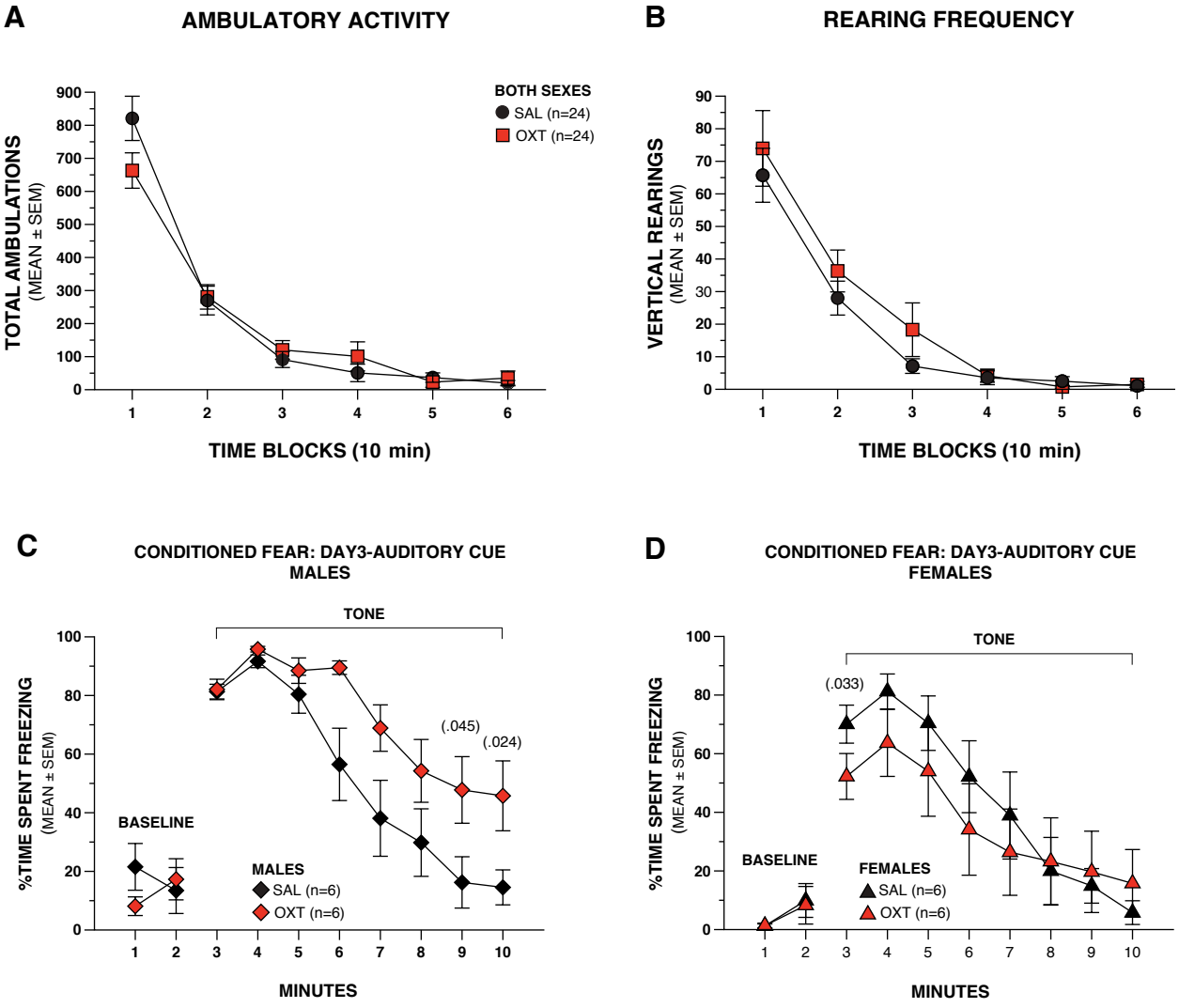

Supplementary Figure 2: The OXT and SAL offspring exhibited similar levels of ambulatory activity/exploration in the open field, but the male OXT offspring rats showed significantly greater freezing levels during auditory cue testing. A. No significant effects involving Treatment were observed for total ambulations (whole body movements) in the open field, although a significant Sex effect was found (p=0.020). However, subsequent analyses did not reveal differences between groups within either the male or female offspring rats (not shown). B. No significant effects involving Treatment or Sex were obtained as a result of analyzing the data for vertical rearing frequency in the open field. C. No significant differences in freezing were found between the male offspring groups during the altered context baseline on day 3. However, the male OXT offspring displayed significantly higher freezing levels during the presentation of the auditory cue (tone) compared to the male SAL offspring (Treatment effect: *p=0.027). Moreover, large differences were observed during minutes 9 (p=0.045) and 10 (p=0.024), although these comparisons were

not significant according to Bonferroni correction ($p<0.007$). D. No significant effects involving Treatment or Sex were found as a result of analyzing the female baseline or auditory cue data.

3. Taqman qPCR for OXTR gene expression in the fetal brain

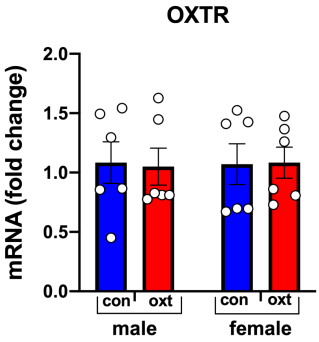

Supplementary figure 3: To ensure that the changes observed in the fetal brain at E21 following OXT bolus in the dam was due to placental ischemia-hypoxia and not due to direct engagement with OXT receptor, we performed TaqMan® qPCR with a pre-validated OXTR probe. We observed neither treatment nor sex differences in the expression of OXTR gene in the fetal cortex. This provided reassurance that the observed changes were not due to direct OXTR activation. Data analyzed with 2-way ANOVA and presented as mean ± SEM; Treatment: F (1, 20) = 0.013 p=0.9114, Sex: F (1, 20) = 0.016 p=0.8993, Treatment x Sex Interaction: F (1, 20) = 0.025 p=0.8767.

4. Western blotting for HIF1a and CC3

Nuclear HIF1a protein expression at 1 h

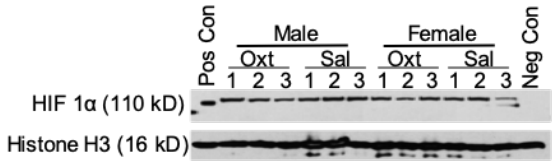

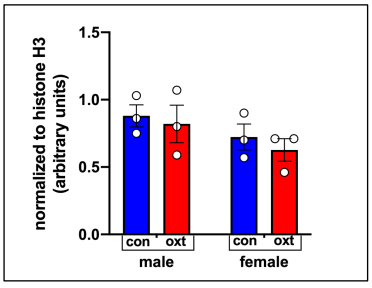

Transient OXT-induced hypercontractility does not increase nuclear hif1a protein expression in the developing fetal brain. E21 fetal brains from both male and female pups were collected 18 h after OXT (100 mcg/kg) or saline (n=3 dams/treatment with one pup of either sex/dam). Hif1a protein expression in the nucleus, normalized to histone H3, was not different between groups. Data analyzed with 2-way ANOVA and presented as mean ± SEM; Treatment: F (1, 8) = 0.58, p=0.47, Sex: F (1, 8) = 2.9, p=0.13, Treatment x Sex Interaction: F (1, 8) = 0.03, p=0.86.

Cleaved caspase-3 protein expression at 18 h

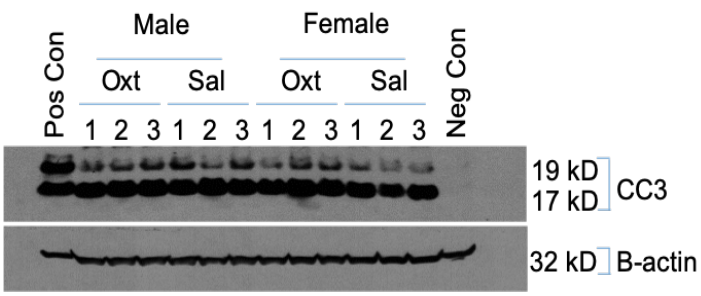

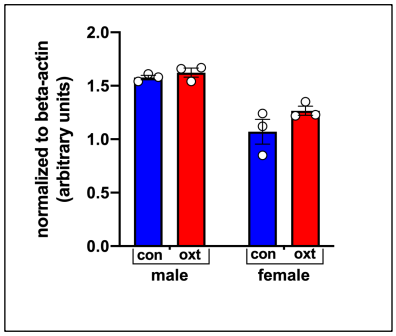

Transient OXT-induced hypercontractility does not induce apoptosis in the developing fetal brain. E21 fetal brains from both male and female pups were collected 18 h after OXT (100 mcg/kg) or saline (n=3 dams/treatment with one pup of either sex/dam). Cleaved caspase-3 protein expression, normalized to beta-actin, was not different between groups, though the overall level of cc3 expression was significantly lower in females of both treatment conditions. Data analyzed with 2-way ANOVA and presented as mean ± SEM; Treatment: $F(1, 8) = 3.4$, $p=0.1$, Sex: $F(1, 8) = 43$, ***$p=0.002$, Treatment x Sex Interaction: $F(1, 8) = 1.3$, $p=0.29$.

5. Supplementary FCOIS data from the brain of OXT and saline-exposed P23 male rat offspring